Volume 43A, Issue 1, January 2012　　　　　　ISSN 1359-835X

ELSEVIER

composites

Part A: applied science and manufacturing

http://www.elsevier.com/locate/compositesa

Available online at www.sciencedirect.com

SciVerse ScienceDirect

(This is a sample cover image for this issue. The actual cover is not yet available at this time.)

Carbon fiber polymer–matrix structural composites exhibiting greatly enhanced through-thickness thermoelectric figure of merit

Seungjin Han [1], D.D.L. Chung *

Composite Materials Research Laboratory, University at Buffalo, State University of New York, Buffalo, NY 14260-4400, USA

ABSTRACT

The through-thickness thermoelectric behavior of continuous carbon fiber epoxy-matrix composites is greatly improved by adding tellurium particles (13 vol.%), bismuth telluride particles (2 vol.%) and carbon black (2 vol.%). The thermoelectric power is increased from 8 to 163 μV/K, the electrical resistivity is decreased from 0.17 to 0.02 Ω.cm, the thermal conductivity is decreased from 1.31 to 0.51 W/m.K, and the dimensionless thermoelectric figure of merit ZT at 70 °C is increased from 9×10^{-6} to 9×10^{-2}. Tellurium increases the thermoelectric power greatly. Bismuth telluride decreases the electrical resistivity and thermal conductivity. Carbon black decreases the electrical resistivity.

© 2013 Elsevier Ltd. All rights reserved.

1. Introduction

1.1. Thermoelectric energy generation

Energy harvesting refers to the conversion to electricity of various forms of energy (mechanical, thermal, light, etc.) that is present in the environment anyway. The efficiency and cost of the energy conversion and the abundance of the particular form of energy determine the practicality of large-scale energy harvesting, which is an avenue to alleviate the energy crisis and reduce the negative environmental impact of the burning of fossil fuels. This paper is concerned with thermoelectric conversion of thermal energy to electricity.

Thermal energy is commonly available in the environment due to waste heat from various devices (e.g., engines, hot gas exhausts, reactors, furnaces, heaters, boilers, hot water pipes, friction sources, machinery, integrated circuits, lights and lasers) and due to natural heating by the sun. These sources of energy are little used in practice, due to the shortcomings and limitations of conventional technologies for the required energy conversion. The conversion of thermal energy to electricity provides clean energy and can use thermal energy that is largely untapped.

The conversion of thermal energy to electricity is commonly conducted by using the thermoelectric effect, in which a temperature gradient in a material results in a voltage difference between the points in the material that are at different temperatures. The effect is also known as the Seebeck effect. The severity of this effect is described by the thermoelectric power (also known as the Seebeck coefficient), which is defined as the voltage difference per unit temperature difference between two points in the material. In general, the negative end of the voltage difference can be at the hot point or the cold point of the temperature gradient. A material that exhibits a substantial thermoelectric effect is known as a thermoelectric material. Examples of thermoelectric materials are bismuth, tellurium, bismuth telluride, lead telluride, zinc antimonide, germanium and silicon.

The effectiveness of a thermoelectric material for energy conversion requires the combination of high thermoelectric power, low electrical resistivity and low thermal conductivity. A low electrical resistivity is needed for a substantial current to pass through the thermoelectric material as the material provides electricity. A low thermal conductivity is needed to provide a substantial temperature gradient in the material.

The figure of merit (Z) of a thermoelectric material is given by

$$Z = S^2/(\rho k), \tag{1}$$

where S is the Seebeck coefficient, ρ is the electrical resistivity and k is the thermal conductivity. The unit of Z is K^{-1}. The dimensionless figure of merit (ZT) is given by the product of Z and the temperature T in K, where T is the average temperature in the presence of a temperature gradient. The ZT value relates to the thermodynamic efficiency.

State-of-the-art thermoelectric materials in bulk form have *ZT* values about 1.2 at room temperature. Thin-film thermoelectric materials can reach higher *ZT* values, because thin films can allow quantum confinement of the carrier, thereby obtaining an enhanced density of states near the Fermi energy. In addition, thin films can allow structures in the form of superlattices with interfaces that block phonons but transmit electrons. For practical application, bulk thermoelectric materials are needed, since the thickness of a thin film is too small to support a substantial temperature difference. Thus, the state of the art of thermoelectric materials is not adequate for practical large-scale conversion of thermal energy to electrical energy.

Prior work [1–13] used various techniques to raise *ZT*, with particular attention given to the decrease of both the thermal conductivity and the electrical resistivity. The techniques include the formation of thermoelectric materials in the form of alloys (e.g., PbTe–Ge [1], La-doped PbTe [2], $Pb_{0.75}Sn_{0.25}Te$ [3], nanocrystalline compounds (e.g., Bi_2Te_3 [4]), nanostructured alloys (e.g., bismuth–antimony–tellurium [5] and silicon–germanium [6]), oxides (e.g., perovskites [7] and $La_{0.8}Sr_{0.2}Co_{1-x}Mn_xO_3$ [8]), skutterudites [9], AgTlTe [10], half-Heusler compounds [11], composites (e.g., $ZrO_2/CoSb_3$ [12]) and copolymers [13]. In particular, interfaces have been used to reduce the thermal conductivity.

For large-scale thermoelectric energy conversion, it is important to have thermoelectric materials that can be formed into large bulk cost-effective devices, as needed to capture a large amount of thermal energy in practical cost-effective implementation of the energy harvesting technology. As the electrical resistance is inversely proportional to the area perpendicular to the resistance direction, a large area of the thermoelectric material in the plane perpendicular to the temperature gradient is valuable for providing a small resistance and hence a high electric power. A large area and a high *ZT* value are both valuable. Prior work has focused on raising *ZT*, with little attention on increasing the area. All the techniques mentioned in the last paragraph suffer from problems associated with one or more of the following: high costs of materials and processing, thermoelectric material size limitation, production scale-up difficulty, insufficiently high *ZT* values, inadequate mechanical performance, and implementation difficulty. In particular, many of the techniques involve thermoelectric materials in the form of films, which are not suitable for practical use.

1.2. Structures capable of energy harvesting

An energy harvesting approach that differs that those of prior work [1–13] involves modification of a structural material that is not capable of energy harvesting but is widely available in large scale, such that the modification renders the material energy harvesting ability. This approach results in a multifunctional structural material that can provide both structural and thermoelectric functions. Such a multifunctional material enables self-powered structures, i.e., structures that generate electric power. Self-powering is attractive for structures for which the use of batteries is not desired, structures to which power transmission lines cannot reach, and strategic structures that require back-up energy.

The rendering of the energy harvesting function to a structure by using a structural material that has this inherent ability is to be distinguished from the rendering that involves embedded or attached devices. The latter method [14] suffers from high cost, poor durability (particularly for attached devices), mechanical property loss (in case of device embedment) and limited functional volume.

The developing of structural materials that have the inherent ability to harvest energy is challenging from a scientific viewpoint, since the structural material needs to be modified in such a way as to provide this function. In addition, for structural performance, the mechanical properties should not be degraded by the modification.

In case of structural materials in the form of composites with continuous fiber reinforcement, the volume fraction of the continuous fibers in the composite must be sufficiently high after the modification, since the fibers are the load-bearing component. Furthermore, for good mechanical performance, the bond between fiber and polymer matrix must be sufficient after the modification.

1.3. Carbon fiber polymer–matrix structural composites

Continuous carbon fiber epoxy-matrix composites are widely used for aircraft, satellites, missiles, windmills and other light-weight structures. A carbon fiber polymer–matrix composite commonly comprises layers of fibers that are in one or more directions that are all in the plane of each layer. Each layer has a large number of fibers in the plane of the layer and there are a substantial number of fibers within the thickness of a layer. Each fiber layer is known as a lamina or a ply. Due to the in-plane orientation of the fibers, the in-plane electrical conductivity of the composite is much higher than that in the direction perpendicular to the laminae. The direction perpendicular to the laminae is known as the through-thickness direction of the composite.

Although polymers that are inherently conductive in the absence of fillers are available, most cost-effective polymers are not conductive. Due to (i) the slight waviness of the fibers in a typical carbon fiber composite, and (ii) the incomplete or imperfect coverage of a fiber by the polymer matrix in a composite, fiber–fiber contact points exist in a composite, thus resulting in electrical conductivity in the through-thickness direction of a conventional carbon fiber polymer–matrix composite, even when the polymer matrix itself is nonconductive. Therefore, the composite is conductive in both in the in-plane direction and the through-thickness direction. In other words, the composite does not have insulating character in any direction.

The interlaminar interface in a continuous fiber composite is the interface between adjacent lamellae in the composite. This interface is particularly distinct when the fibers in the adjacent lamellae are oriented in different directions. Fiber–fiber contact points normally exist across the interlaminar interface. Therefore, in spite of the presence of one or more interlaminar interfaces in a typical carbon fiber composite, the composite is not insulating in the through-thickness direction.

Thermoelectric particles have been incorporated in carbon fiber polymer–matrix composites for enhancing the thermoelectric power [16,17]. The effect of the thermoelectric particle incorporation is much smaller for the thermoelectric power in the longitudinal (fiber) direction than the through-thickness direction of the composite, due to the dominance of the carbon fibers in governing the longitudinal effect [16]. Therefore, this paper is focused on the thermoelectric behavior in the through-thickness direction.

Carbon fiber is an electrical conductor that is very weakly thermoelectric [15]. The incorporation of thermoelectric particles (such as tellurium and bismuth telluride) at the interlaminar interface of a carbon fiber polymer–matrix composite increases the thermoelectric power substantially [16,17]. The incorporation of tellurium particles causes the thermoelectric power to be strongly positive, whereas the incorporation of bismuth telluride particles causes the thermoelectric power to be strongly negative [16,17]. The greater is the tellurium content, the higher is the magnitude of the thermoelectric power [17]. A mixture of tellurium and bismuth telluride particles gives greater enhancement of the thermoelectric power than the use of a single type of thermoelectric particle [16]. The highest value of the absolute thermoelectric power reported for carbon fiber polymer–matrix composites is +110 µV/K, which is the value for a composite with tellurium as the sole interlaminar filler [17]. However, the *ZT* value, the electrical resistivity and the thermal conductivity were not reported in the prior work [16,17].

A decrease in curing pressure decreases the magnitude of the thermoelectric power [17] and decreases the through-thickness thermal conductivity [18]. Furthermore, as suggested by the interlaminar interface thickness increase [18], the lamina thickness increase [18] and the interlaminar interface contact electrical resistivity increase [19], increase in the through-thickness electrical resistivity is expected. However, the effect of curing pressure on ZT has not been previously reported.

The modification of continuous fiber polymer–matrix composites by the incorporation of fillers can be conducted by introduction of the filler to the interlaminar interface region of the composite [16,17] or introduction of the filler to the matrix (or the matrix precursor, such as the epoxy resin) prior to combining the continuous fibers with the matrix [20]. The latter method suffers from the increase of the viscosity of the resin after addition of the filler and the consequent difficulty of the resin to flow for the purpose of obtaining a fiber–matrix interface that has little or no voids. Therefore, this work uses the former method of filler introduction.

The interlaminar interface region is a region that is relatively rich in the matrix. In order to avoid excessive thickness of the interface region after filler incorporation (so as to avoid excessive reduction of the continuous fiber volume fraction), the amount of matrix material in the interface region may be reduced. The reduction of the interfacial matrix material may be achieved by the application of a liquid-based filler dispersion on the prepreg surface (i.e., the surface of a sheet of unidirectional continuous fiber, such that the matrix or matrix precursor, along with the curing agent, if needed, has been impregnated into the sheet), such that the liquid is able to dissolve the matrix or matrix precursor. This dissolution causes partial removal of the excessive matrix or matrix precursor on the prepreg surface. By controlling the time of contact of the dispersion with the prepreg surface, the extent of matrix (or matrix precursor) removal by dissolution is limited. On the other hand, the liquid must be allowed to evaporate thoroughly from the prepreg surface after application, in order to avoid the presence of voids in the composite. In addition, the liquid must be able to disperse the filler. In this work, the liquid is ethylene glycol monoethyl ether (EGME), which has been previously shown to be effective [21].

The use of carbon black as an interlaminar filler increases the through-thickness thermal conductivity of carbon fiber epoxy-matrix composites [21] and has little effect on the thermoelectric power [17]. The effect of carbon black on the electrical resistivity and ZT has not been previously reported.

The addition of carbon black increases slightly the magnitude of the thermoelectric power, whereas the addition of tellurium or bismuth telluride greatly increases this magnitude (Table 1) [17]. Tellurium causes the thermoelectric power to be very positive, whereas bismuth telluride causes the thermoelectric power to be very negative (Table 1) [17]. In other words, tellurium and bismuth telluride give opposite effects. That tellurium and bismuth telluride as interlaminar fillers give opposite signs of the thermoelectric power of the laminate has been previously reported [15]. This re-

flects the difference in inherent thermoelectric behavior of bismuth telluride and tellurium and supports the notion that the interaction between the filler and the carbon fibers involves the thermoelectric nature of the filler. A possible mechanism of the interaction involves the carriers flowing in the thermoelectric filler due to the high thermoelectric power of the filler spreading to the neighboring electrical conductor, namely the laminae.

Reducing the amount of tellurium by a factor of 2 decreases the thermoelectric power by about a factor of 2 (Table 1) [17]. This further supports the notion that the thermoelectric filler interacts with the laminae. In spite of the fact that the majority of the tellurium resides at the interlaminar interface, a minority of the tellurium penetrates the laminae to a limited extent [17]. The filler penetration is expected to increase the degree of waviness of the fibers; more waviness results in more contact points among the fibers in the through-thickness direction. The contact points enable electrons to hop from one fiber to another [17–19].

The combined use of tellurium and carbon black as interlaminar fillers gives lower (less positive) thermoelectric power than the use of tellurium as the sole filler (Table 1) [17], probably due to the lower proportion of tellurium when carbon black is present. Carbon black is a highly compressible and conformable solid, due to its being in the form of porous aggregates of nanoparticles. Hence, carbon black is expected to have less geometric effect than tellurium or bismuth telluride particles, which are not conformable and are relatively large in particle size.

1.4. Thermoelectric composites science

Composites science has long been addressed in terms of the density, elastic modulus, electrical resistivity and thermal conductivity. Various models, including the Rule of Mixtures, have long been provided to calculate the composite properties based on the properties and proportions of the constituents, such as the fibers and the matrix. However, composites science is little developed in relation to the thermoelectric power.

Interfaces are present in essentially all practical materials. Prior work on thermoelectric materials has addressed the effect of interfaces on the thermal conductivity and the electrical resistivity, but essentially not on the effect of interfaces on the thermoelectric power. A recent research breakthrough [17] has allowed the interface and bulk contributions to the thermoelectric power of a material to be decoupled for the first time, thus quantifying the effect of the interface and discovering the carrier backflow that occurs at the interface. The backflow, which is not desirable, is not a true thermoelectric effect, but the forward flow in the bulk is.

The method [17] of decoupling the lamina and interlaminar interface contributions to the Seebeck voltage is by testing composites that are identical other than the number of laminae. The specimen voltage consists of the voltages from all the laminae and those from all of the interlaminar interfaces in the laminate. Hence, for the 15-lamina laminate, which consists of 15 laminae and 14 interlaminar interfaces,

$$V_{s,15} = 15V_\ell + 14V_i, \tag{2}$$

where V_ℓ is the voltage across the thickness of a lamina and V_i is the voltage across the thickness of an interlaminar interface region. Similarly, for the 30-lamina laminate, which consists of 30 laminae and 29 interlaminar interfaces,

$$V_{s,30} = 30V_\ell + 29V_i. \tag{3}$$

Solution of Eqs. (2) and (3) under the condition that the temperature gradient is essentially the same for the 15-lamina and 30-lamina composites gives V_ℓ and V_i.

The abovementioned breakthrough [17] was made using a continuous PAN-based carbon fiber epoxy-matrix composite laminate

Table 1
Thermoelectric results for crossply laminates made at a curing pressure of 4.0 MPa. CB = carbon black. The data are from the prior work of the present authors [17].

Filler	Thermoelectric power (μV/K)
None	−3.7
CB	−4.1
Te (8 μm), full amount	110
Te (8 μm), half amount	44
Te (2 μm), half amount	60
Bi$_2$Te$_3$ (2 μm), half amount	−50
Te (8 μm) full amount + CB	92

in the through-thickness direction. Thermoelectric power magnitudes at ~70 °C up to 110, 1670 and 11,000 μV/K were obtained for the laminate, each lamina and each interlaminar interface respectively. The interlaminar interface provides an apparent (not true) thermoelectric effect due to carrier backflow. The interfacial voltage is opposite in sign from both the laminate and lamina voltages and is slightly lower in magnitude than the lamina voltage. The resistance-related voltage at each electrical contact was decoupled from the thermoelectric specimen voltages [17].

Although interfaces tend to reduce the thermal conductivity, they also tend to reduce the thermoelectric power and increase the electrical resistivity. Therefore, interface engineering is critical to the development of thermoelectric materials.

1.5. Objectives

This paper is aimed at evaluating and increasing the ZT of carbon fiber polymer–matrix composites. A secondary objective is to study the effects of the curing pressure and interlaminar fillers on ZT. The fillers include tellurium particles, bismuth telluride particles and carbon black. Filler combinations are also used to attain high ZT, as different fillers can have synergistic effects on the thermoelectric power, electrical resistivity and thermal conductivity.

2. Experimental methods

2.1. Materials

A unidirectional carbon fiber epoxy prepreg from Tencate Advanced Composites USA, Inc., Morgan Hill, CA, is used. Its carbon fiber, designated Torayca M46JB, is in the form of 12 K PAN-based fiber, with tensile modulus 436 GPa, tensile strength 4.0 GPa, fiber diameter 5.0 ± 0.3 μm (measured in this work), and elongation at break 1.0%. Its resin is RS-36 epoxy. The prepreg has areal mass 168 ± 5 g/m^2 and resin content 33 ± 2 wt.%. Curing is conducted at 177 °C for 90 min, as recommended by the prepreg manufacturer. The curing pressure is 4.0 MPa, unless noted otherwise.

The interlaminar fillers used are tellurium particles, bismuth telluride particles and carbon black. The tellurium particles with density 6.24 g/cm^3 and purity 99.5% are obtained from Electro-Optic Materials, Advanced Materials, Umicore Group, Hoboken, Belgium; the average particle size has been reduced by ball milling in this work to either 8 or 2 μm. The bismuth telluride (Bi$_2$Te$_3$) particles with density 7.7 g/cm^3 and purity 99.99% are obtained from CERAC, Inc., Milwaukee, WI; the average particle size has been reduced by ball milling in this work to 2 μm.

The carbon black is Vulcan XC72R GP-3820 from Cabot Corp., Billerica, MA. It is a powder with particle size 30 nm, a nitrogen specific surface area 254 m^2/g, maximum ash content 0.2%, volatile content 1.07%, and density 1.7–1.9 g/cm^3. Furthermore, this carbon black is not pelleted, so that the fluffiness enhances the dispersibility.

2.2. Composite fabrication

Three fillers are used as sole fillers, namely carbon black, tellurium and bismuth telluride. Only one filler combination is used, namely a mixture of tellurium and carbon black at a volume ratio of 7:1; the mixture is obtained by using a ball mill (rolling in the absence of grinding balls in the container) for 2 h.

In case of carbon black as the sole filler, the carbon black is applied to the prepreg surface by immersion of the prepreg in the EGME-based dispersion containing 0.8 wt.% carbon black for 3 s [21]. In case of fillers involving thermoelectric particles (tellurium or bismuth telluride), the filler (or filler combination) is applied to

the prepreg by brushing (using a paint brush) the corresponding EGME-based dispersion on the prepreg surface. The weight ratio of EGME to the filler (or filler combination) in the dispersion is 1:1. Prior to this brush application of the filler (or filler combination), the prepreg has been immersed in EGME (without filler) for 3 s and subsequently allowed to dry at room temperature for about 24 h. The effectiveness of EGME and the adequacy of its drying have been previously shown [21]. After the abovementioned prepreg modification, the prepreg sheets are stacked in a crossply configuration.

In the unmodified composite, none of the interlaminar interfaces is modified. In a modified composite, all of the interlaminar interfaces are modified.

Specimens for thermoelectric power measurement are 30-lamina composites of size 23×23 mm. Specimens for electrical resistivity measurement are 10-lamina composites of size 20×20 mm. Specimens for thermal conductivity measurement are 2-, 3- and 4-lamina composites of size 1×1 in (25×25 mm), which provide three specimen thicknesses for obtaining the thermal resistivity vs. the thickness. The slope of the resulting line relates to the thermal conductivity [18].

The prepreg stack is cured using a hot hydraulic press (Carver, Inc., Wabash, IN), which provides heat and pressure. The press involves two metal platens for sandwiching a mold containing a prepreg stack and the mating piston above the mold. The mold used has inner dimensions of 4.0×3.0 in (100×76 mm) and wall thickness 0.5 in (13 mm). The piston is a tight-fit to the mold, with dimensions $4.0 \times 3.0 \times 1.0$ in ($100 \times 76 \times 25$ mm). Both the mold and piston are made of steel. The small hole on the bottom side at the center of the mold allows a thermocouple (Type K) to measure the temperature. The thermocouple is fed to a temperature controller (Watlow Electric Manufacturing Company, St. Louis, MO, Series 981C-10CA-ARRR), which controls the curing process temperature (heating, holding at the maximum temperature and then cooling).

2.3. Testing

2.3.1. Microscopy

The microstructure is observed at the cross-section of the composite specimen after mechanical polishing. The cross section is perpendicular to the plane of the laminae. An optical microscope (Nikon Epiphot inverted metallograph) is used.

2.3.2. Electrical resistivity measurement

The DC through-thickness resistivity is measured by using the four-probe method, with four electrical contacts made with silver paint, such that two contacts are on each of two opposite surfaces of dimensions 20×20 mm and they consist of a loop as the current contact and a dot inside the loop as the voltage contact. A Keithley Model 2001 multimeter is used. Each specimen has 10 laminae.

2.3.3. Thermal conductivity measurement

The thermal contact conductance between two 1.0×1.0 in (25×25 mm) copper blocks with a composite specimen between them is measured using the guarded hot plate method, which is a steady-state method of heat flux measurement (ASTM Method D5470). The heat is provided by a 3.0×3.0 in (76×76 mm) copper block that has two embedded heating coils (top block in Fig. 1). During the period of temperature rise, the heating rate is controlled at 3.2 °C/min by using a temperature controller. This copper block was in contact with one of the 1.0×1.0 in copper blocks that sandwich the composite specimen. The 1.0×1.0 in copper blocks have a surface roughness of 15 μm, which translates to a copper-specimen interface undulation amplitude of 15 μm. The cooling in this test is provided by a second 3.0×3.0 in copper block, which
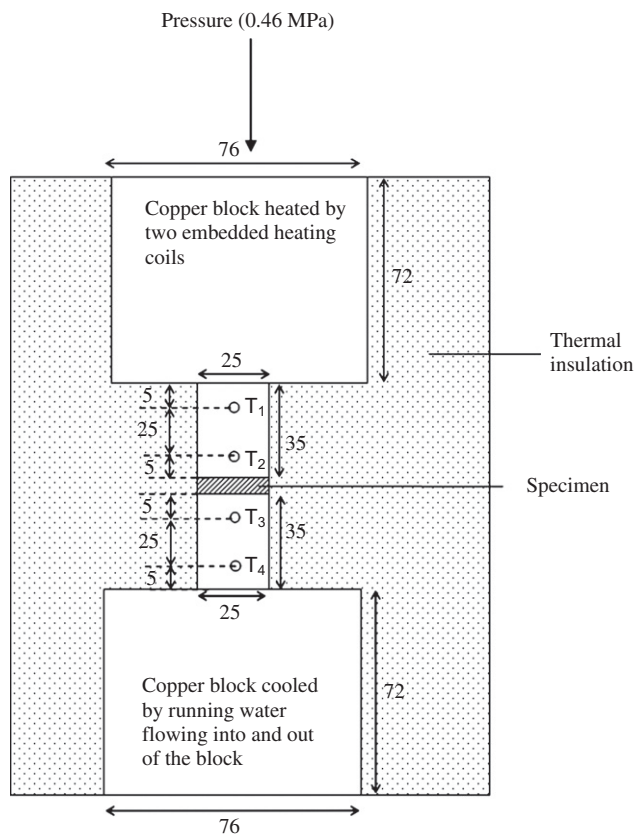
Fig. 1. Set-up for thermal conductivity measurement using the guarded hot plate method. The heat flux is in the direction from the top copper block to the bottom copper block. All dimensions are in mm.

is cooled by running water that flows in and out of the block (bottom block in Fig. 1). This block is in contact with the other 1.0 × 1.0 in copper block that is in contact with the composite specimen. An RTD (resistance thermometer) probe (connected to Digi-Sense ThermoLogR RTD Thermometer from Fisher Scientific Co., with accuracy ±0.03 °C) is inserted in four holes (T_1, T_2, T_3 and T_4 in Fig. 1, each hole of diameter 3.3 mm) one after the other. Two of the four holes are in each of the 1.0 × 1.0 in copper blocks. The temperature gradient is determined from T_1–T_2 and T_3–T_4. These two quantities should be equal at equilibrium, which is attained after holding the temperature of the heater at the desired value for 30 min. Equilibrium is assumed when the temperature variation is within ±0.1 °C in a period of 15 min. At equilibrium, the temperature of the hot block is 100 °C, that of the cold block is in the range 12–25 °C, while that of the top surface of the composite specimen is in the range 76.8–87.0 °C and the bottom surface 36.3–47.3 °C. Thus, the average temperature of the specimen is around 62 °C. The pressure in the direction perpendicular to the plane of the thermal interface is controlled by using a hydraulic press at a pressure of 0.46 MPa. The system is thermally insulated by wrapping laterally all the copper blocks with glass fiber cloth.

In accordance with ASTM Method D5470, the heat flow Q is given by

$$Q = \frac{\lambda A}{d_A} \Delta T, \tag{4}$$

where $\Delta T = T_1 - T_2 = T_3 - T_4$, λ is the thermal conductivity of copper, A is the area of the 1.0 × 1.0 in copper block, and d_A is the distance between thermocouples T_1 and T_2 (i.e., 25 mm).

The temperature at the top surface of the specimen is T_A, which is assumed to be at the mid-point of the composite-copper interface undulation amplitude. This temperature is given by

$$T_A = T_2 - \frac{d_B}{d_A}(T_1 - T_2), \tag{5}$$

where d_B is the distance between thermocouple T_2 and the top surface of the specimen (i.e., 5.0 mm).

The temperature at the bottom surface of the specimen is T_D, which is again assumed to be at the mid-point of the specimen-copper interface undulation amplitude. This temperature is given by

$$T_D = T_3 + \frac{d_D}{d_C}(T_3 - T_4), \tag{6}$$

where d_D is the distance between thermocouple T_3 and the bottom surface of the specimen (i.e., 5.0 mm) and d_C is the distance between thermocouples T_3 and T_4 (i.e., 25 mm).

The two-dimensional thermal resistivity θ is given by

$$\theta = (T_A - T_D)\frac{A}{Q}. \tag{7}$$

Note that insertion of Eq. (4) into Eq. (7) causes cancellation of the term A, so that θ is independent of A.

Each composite is tested at three different thicknesses, with two specimens tested for each thickness. The three thicknesses correspond to 2, 3 and 4 laminae. Two-lamina, three-lamina and four-lamina composites have 1, 2 and 3 interlaminar interfaces respectively. The thermal conductivity (W/m.K) of the composite is the inverse of the slope of the curve of the thermal resistivity vs. thickness.

2.3.4. Thermoelectric power measurement

Evaluation of the through-thickness thermoelectric power involves measuring the voltage between the two opposite surfaces (23 × 23 mm) of a 30-lamina composite when the temperature difference between the two surfaces is increased from 0 to 125 °C. The temperature difference is provided by a pair of copper blocks (1.0 × 1.0 in for each proximate surface), with one block being attached to a resistance-heater metal assembly and the other block being attached to a water-cooled metal assembly, as shown in Fig. 1. The method for measuring the temperature is as described in Section 2.3.3. The voltage is measured by using copper foil that is attached to the specimen surface by using silver paint and that partly protrudes beyond the area of the specimen. In calculating the thermoelectric power, the contribution to the measured voltage by the temperature gradient in the protruded part of the copper foil is removed from the measured voltage.

3. Results and discussion

3.1. Thermoelectric behavior

An increase in the curing pressure increases the thermoelectric power, decreases the electrical resistivity substantially, increases the thermal conductivity slightly, and increases ZT substantially (Table 2). These effects are consistent with the decrease in interlaminar interface thickness due to the increase in the curing pressure [17] and the consequent enhanced through-thickness electronic conduction.

Table 3 shows that carbon black as the sole filler essentially does not affect the thermoelectric power, but decreases the electrical resistivity substantially. This is due to the conformability of the carbon black [22,23], which enhances the electrical connectivity of adjacent laminae.

Table 4 shows that the combined use of tellurium particles (majority filler) and carbon black (minority filler) gives significant increases in the thermoelectric power relative to the case in which carbon black is the sole filler. However, the electrical resistivity is

Table 2
Effect of curing pressure for composites.

Curing pressure (MPa)	Thermoelectric power (μV/K)	Electrical resistivity (Ω.cm)	Thermal conductivity (W/m.K)	ZT at 70 °C
0.5	5.3 ± 0.5	2.95 ± 0.04	1.17 ± 0.02	2.8×10^{-7}
4.0	7.8 ± 1.0	0.171 ± 0.005	1.31 ± 0.01	9.4×10^{-6}

Table 3
Effect of carbon black as the sole filler for composites made at 4.0 MPa curing pressure.

Carbon black	Thermoelectric power (μV/K)	Electrical resistivity (Ω.cm)
No	7.8 ± 1.0	0.171 ± 0.005
Yes	7.0 ± 0.8	0.026 ± 0.002

Table 4
Effect of tellurium particles (2 μm particle size) together with carbon black (CB) at various volume ratios for composites made at 4.0 MPa curing pressure.

Te:CB volume ratio	Thermoelectric power (μV/K)	Electrical resistivity (Ω.cm)
0:1	7.0 ± 0.8	0.026 ± 0.002
7:1	171 ± 8	0.042 ± 0.004
10:1	173 ± 1	0.087 ± 0.003

Table 6
Effect of thermoelectric particles and carbon black (at volume ratio 7:1) for 2 μm thermoelectric particle size and 0.5 MPa curing pressure. The thermoelectric particles consist of tellurium and Bi_2Te_3 at volume ratio 8:1.

Thermoelectric particles and carbon black	Thermoelectric power (μV/K)	Electrical resistivity (Ω.cm)
No	5.3 ± 0.5	2.95 ± 0.04
Yes	83 ± 2	0.96 ± 0.03

increased slightly. Increase in the tellurium to carbon black volume ratio from 7:1 to 10:1 has essentially no effect on the thermoelectric power, but increases the electrical resistivity. Thus, the volume ratio of 7:1 is more effective than that of 10:1.

Table 5 shows that, in the presence of carbon black, increase in the bismuth telluride proportion relative to the tellurium proportion monotonically decreases the thermoelectric power and the electrical resistivity, whether the thermoelectric particle size is 2 or 8 μm. The decrease in the positive thermoelectric power upon increase in the bismuth telluride proportion is consistent with the negative sign of the thermoelectric power when bismuth telluride is present as the sole filler [17]. As shown for the case of the 8 μm thermoelectric particle size, the thermal conductivity decreases monotonically and ZT increases monotonically as the bismuth telluride proportion increases. This trend in ZT is due to the decrease in both electrical resistivity and thermal conductivity, in spite of the slight decrease in thermoelectric power. Thus, the highest ZT is provided by the 8:1 volume ratio of tellurium to bismuth telluride (i.e., the highest proportion of bismuth telluride in case that the tellurium particle size is 8 μm).

At the same ratio of tellurium to bismuth telluride, increase of the thermoelectric particle size from 2 to 8 μm increases the thermoelectric power and decreases the electrical resistivity slightly (Table 5). The use of tellurium and bismuth telluride in the volume ratio of 8:1, with the thermoelectric particle size at 8 μm, gives the best overall performance (high thermoelectric power, low electrical resistivity, low thermal conductivity and high ZT) among all the cases in Table 5. Comparison of Tables 3 and 5 shows that

the addition of tellurium (8 μm) to a composite that contains carbon black greatly increases the thermoelectric power from 7 to 174 μV/K, though the electrical resistivity is increased from 0.026 to 0.038 Ω.cm.

Table 6 shows that, for a curing pressure of 0.5 MPa, the combined use of tellurium, bismuth telluride and carbon black is effective for increasing the thermoelectric power substantially and decreasing the electrical resistivity substantially. This is consistent with the results in Table 5, which is for a curing pressure of 4.0 MPa. Hence, the beneficial effect of this combined use occurs, whether the curing pressure is 0.5 or 4.0 MPa. However, comparison of the results of Tables 5 and 6 indicates that the higher curing pressure gives higher thermoelectric power and lower electrical resistivity. This effect of the curing pressure is consistent with the results in Table 2.

In the presence of carbon black, for the same volume ratio of tellurium to bismuth telluride, the thermoelectric particle size affects the thermoelectric power, such that the thermoelectric power is increased when the thermoelectric particle size is increased from 2 to 8 μm, but is decreased when the particle size is further increased to 18 μm and beyond (Table 7). The electrical resistivity is also affected by the thermoelectric particle size, such that the particle size of 8 μm gives the lowest resistivity. Thus, for high thermoelectric power as well as low resistivity, the particle size of 8 μm is most effective. In contrast, it was previously reported that, in the absence of carbon black, 2 μm tellurium particles give higher thermoelectric power than 8 μm tellurium particles [17]. This means that the optimum thermoelectric particle size depends on whether carbon black is present or not. Due to its conformability, carbon black can fill small spaces, thereby reducing the need for small thermoelectric particles.

That the optimum particle size is around 8 μm in the presence of carbon black is attributed to its approximate match with the interlaminar interface thickness of the unmodified composite. A larger size (18 μm) causes the interface thickness to be large, thereby increasing the electrical contact resistivity of this interface.

Table 5
Effect of Te:Bi_2Te_3 volume ratio for composites made at 4.0 MPa curing pressure. The thermoelectric particles and carbon black are at volume ratio 7:1.

Thermoelectric particle size (μm)	Te:Bi_2Te_3 volume ratio	Thermoelectric power (μV/K)	Electrical resistivity (Ω.cm)	Thermal conductivity (W/m.K)	ZT at 70 °C
2	1:0	171.3 ± 8.0	0.042 ± 0.004	/	/
2	12:1	153.3 ± 7.0	0.030 ± 0.001	/	/
2	8:1	137.8 ± 6.5	0.023 ± 0.001	/	/
2	4:1	85.4 ± 4.1	0.020 ± 0.002	/	/
8	1:0	174.3 ± 4.0	0.038 ± 0.002	1.35 ± 0.001	0.020
8	12:1	167.3 ± 2.0	0.023 ± 0.001	1.21 ± 0.001	0.035
8	8:1	163.3 ± 5.5	0.021 ± 0.001	0.511 ± 0.003	0.086

Table 7
Effect of thermoelectric particle size for composites made at 4.0 MPa curing pressure. The thermoelectric particles and carbon black are at volume ratio 7:1. The thermoelectric particles consist of tellurium and Bi_2Te_3 at volume ratio 8:1 and 12:1.

Te:Bi_2Te_3 volume ratio	Thermoelectric particle size (μm)	Thermoelectric power (μV/K)	Electrical resistivity (Ω.cm)	Thermal conductivity (W/m.K)	ZT at 70 °C
8:1	2	137.8 ± 6.5	0.023 ± 0.001	/	/
8:1	8	163.3 ± 5.5	0.021 ± 0.001	0.511 ± 0.003	0.086
8:1	18	117.4 ± 6.4	0.032 ± 0.002	/	/
8:1	28	93.7 ± 4.7	0.033 ± 0.001	/	/
12:1	2	153.3 ± 7.0	0.030 ± 0.001	/	/
12:1	8	167.3 ± 2.0	0.023 ± 0.001	1.21 ± 0.001	0.035

A smaller size (2 μm) may cause more than one thermoelectric particle to be stacked along the thickness of the interlaminar interface, thus increasing the contact electrical resistivity of this interface through the presence of additional interfaces, such as the interface between thermoelectric particles and the interface between a thermoelectric particle and the polymer matrix.

The combination of tellurium particles and bismuth telluride particles in the volume ratio of 8:1, along with carbon black, such that the volume ratio of the thermoelectric particles (tellurium plus bismuth telluride) to carbon black is 7:1, for a curing pressure of 4.0 MPa, causes the thermoelectric power to increase from 8 to 163 μV/K, while the electrical resistivity is decreased from 0.17 to 0.02 Ω.cm, the thermal conductivity is decreased from 1.31 to 0.51 W/m.K, and ZT is increased from 9×10^{-6} to 9×10^{-2}, as shown by comparing Tables 2 and 7. Fig. 2 shows the variation of the Seebeck voltage with the temperature difference for this thermoelectric composite. The curve is close to being linear. The average slope is taken as the thermoelectric power. The hysteresis is negligible. Fig. 3 shows the variation of the thermal resistivity with specimen thickness for this thermoelectric composite; the slope of this curve relates to the thermal conductivity.

The highest ZT achieved in this work is 0.086, which is for the case of tellurium and bismuth telluride at 8:1 in volume ratio and these thermoelectric particles and carbon black at 7:1 volume ratio.

This ZT value corresponds to $Z = 2.5 \times 10^{-4}$ K^{-1}. This Z value is higher than the value of 10^{-5} K^{-1} reported for boron and boron phosphide films [24], the value of $(3.4–4.8) \times 10^{-5}$ K^{-1} reported for sintered $Bi_2Sr_2Ca_{1-x}Y_xCu_2O_y$ ($x = 0.8$) [25], the value of 1.07×10^{-4} K^{-1} reported for (Bi, Pb)–Sr–Co–O oxide [26], the value of 1.3×10^{-4} K^{-1} reported for $(Pr_{0.9}Ca_{0.1}) CoO_3$ [27] and the value of 1.5×10^{-4} K^{-1} reported for both perovskite-type rare-earth cobalt oxides [28] and Me-substituted $In_4Sn_3O_{12}$ (Me = Y and Ti) [29], but is lower than the value of 7.65×10^{-4} K^{-1} reported for Mn–Si [30], the value of 8.4×10^{-4} K^{-1} reported for $Bi_{85}Sb_{15}$ solid solution [31], the value of $(1.0–1.1) \times 10^{-3}$ K^{-1} reported for $Pb_{1-x}Sn_xTe$:Te solid solutions [32], the value of 2.31×10^{-3} K^{-1} reported for both n-type $(Bi_2Se_3)_x(Bi_2Te_3)_{1-x}$ [33] and $(Bi_2Se_3)_{0.05}(Bi_2Te_3)_{0.95}$ [34], the value of 2.6×10^{-3} K^{-1} reported for β-Ag_2Se [35] and the value of 3×10^{-3} K^{-1} reported for p-type $(Bi_2Te_3)_x(Sb_2Te_3)_{1-x}$ [36].

The highest ZT value of 0.086 obtained in this work is higher than that of the corresponding unmodified composite by four orders of magnitude. It is also higher than the value of 0.011 reported for polyaniline films [37] and the value of 0.035 reported for the composite crystal $[Ca_2CoO_{3.34}]_{0.614}[CoO_2]$ [38]. However, it is lower than the value of 0.1 reported for $Yb_yCo_4Sn_xSb_{12-x}$ skutterudites [39], the value of 0.12 reported for Ge_xNbTe_2 [40], the value of 0.15 reported for $Fe_xCr_{3-x}Se_4$ [41], the value of 0.5 reported for $Bi_{2(1-x)}In_{2x}Te_3$ [42], the value of 0.54 reported for B-C-Y system composites [43], the value of 0.65 reported for chalcogenide systems [44], the value of 0.78 reported for sintered $NaCo_2O_4$ [45], the value of 0.8 reported for both $CsBi_4Te_6$ [46] and thallium-filled skutterudites [47], the value of 0.9 reported for both n-type $Si_{0.95}Ge_{0.05}$ [48] and quantum-dot superlattices [49], the value of
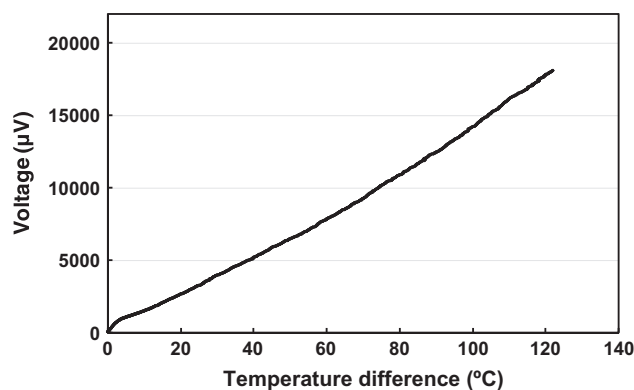

Fig. 2. Seebeck voltage (without correction for the copper wire) vs. the temperature difference during heating for the thermoelectric carbon fiber composite that exhibits the highest ZT value of 0.086 and contains tellurium and bismuth telluride at 8:1 in volume ratio and thermoelectric particles and carbon black at 7:1 volume ratio.

Fig. 3. Variation of the thermal resistivity with the composite thickness for the composite that exhibits the highest value of ZT value of 0.086 and contains tellurium and bismuth telluride at 8:1 in volume ratio and thermoele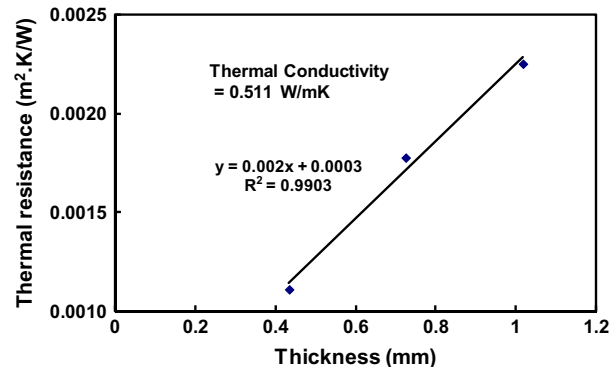ctric particles and carbon black at 7:1 volume ratio. Data points are provided for three thicknesses, which correspond to composites with 2, 3 and 4 laminae. The thermal conductivity is equal to the reciprocal of the slope of the plot.

nearly 1 reported for $Co_{0.88}Pt_{0.12}Sb_3$ [50], the value of 1 reported for both $Yb_{0.19}Co_4Sb_{12}$ [51] and Yb-filled skutterudites [52] and the value of 1.1 reported for $Ba_{0.3}Co_4Sb_{12}$ [53].

The relatively low ZT value achieved in this work is partly due to the relatively low temperature of 70 °C. The low temperature is a consequence of the inability of a polymer–matrix composite to withstand high temperatures. Nevertheless, this work provides a basis for further development of structural thermoelectric composites.

3.2. Structure

Table 8 shows the density and component volume fractions of the unmodified and modified composites. The components are

Table 8

Composite density and component volume fractions and of carbon fiber epoxy-matrix composites made at a curing pressure of 4.0 MPa.

ZT	Composite density (g/cm^3)	Interlaminar interface thickness (μm)	Volume fraction					
			Continuous fiber	Matrix	Filler			
					CB	Te	Bi$_2$Te$_3$	Total
9.4×10^{-6}	1.650 ± 0.027	2.6 ± 1.5	0.688 ± 0.044	0.312 ± 0.044	0	0	0	0
2.9×10^{-5}	1.664 ± 0.033	2.8 ± 1.7	0.681 ± 0.005	0.286 ± 0.005	0.033 ± 0.002	0	0	0.033 ± 0.002
2.0×10^{-2}	2.160 ± 0.074	17.0 ± 3.8	0.531 ± 0.002	0.308 ± 0.002	0.019 ± 0.001	0.142 ± 0.002	0	0.161 ± 0.003
8.6×10^{-2}	2.236 ± 0.095	18.0 ± 3.6	0.534 ± 0.002	0.305 ± 0.006	0.020 ± 0.001	0.126 ± 0.006	0.016 ± 0.001	0.162 ± 0.008

the continuous carbon fiber, the filler(s) and the matrix. The volume fractions of the fiber and matrix are calculated from the measured density, based on the Rule of Mixtures. The volume fraction of a filler is obtained by dividing the volume of the filler by the volume of the composite, with the volume of the filler obtained by dividing the mass of the filler by the density of the filler. The mass

Fig. 4. Optical microscope photographs of the mechanically polished cross section of crossply carbon fiber epoxy-matrix composites fabricated at a curing pressure of 4.0 MPa. (a) Unmodified composite. (b) Modified composite that exhibits the highest ZT value of 0.086 and contains tellurium and bismuth telluride at 8:1 in volume ratio and thermoelectric particles and carbon black at 7:1 volume ratio. The interlaminar thickness is 2.6 ± 1.5 μm and 18.0 ± 3.6 μm in (a) and (b) respectively. The two laminae shown are 90° apart in the fiber orientation. The bottom lamina has fibers perpendicular to the page, with the fiber ends shown as grey circles. The top lamina has fibers in the plane of the page, with the fibers shown as long grey regions.

of the filler is obtained by subtracting the mass of the prepreg (3.0×3.0 cm) that has been treated by the solvent without introduction of this filler (either as the sole filler or an additional filler) from the mass of the prepreg that has been treated by the solvent with introduction of this filler. For example, Bi$_2$Te$_3$ is the additional filler relative to the composite that contains carbon black and Te.

The fiber volume fraction is decreased by the presence of tellurium particles, but is essentially not affected by the presence of carbon black, the volume fraction of which is much lower than that of the tellurium. The composite density is increased by the presence of thermoelectric particles, but is essentially not affected by the presence of carbon black.

The filler combination corresponding to the composite that exhibits the highest ZT value of 0.086, i.e., tellurium particles (12.6 vol.% of composite) and bismuth telluride particles (1.6 vol.% of composite) at 8:1 in volume ratio and these thermoelectric particles and carbon black (2.0 vol.% of composite) at 7:1 volume ratio, causes the interlaminar interface thickness to increase from 3 to 18 μm (Table 8 and Fig. 4) and causes the carbon fiber content to decrease from 69 to 53 vol.%. Since the carbon fiber is the primary reinforcement, this decrease in the fiber content is estimated to decrease the elastic modulus of the composite by 23%, based on the Rule of Mixtures. Future work should be directed at minimizing the thermoelectric particle volume fraction so as to minimize the modulus decrease. The thickness of a lamina is essentially not affected by the fillers. The fibers of the adjacent laminae of the composite that exhibits the highest ZT are not in contact (Fig. 4).

4. Conclusion

The through-thickness thermoelectric behavior of carbon fiber epoxy-matrix composites is greatly improved by modification of the interlaminar interface through filler incorporation. At a curing pressure of 4.0 MPa, by using tellurium particles (12.6 vol.% of composite) and bismuth telluride particles (1.6 vol.% of composite) at a volume ratio of 8:1 and using these thermoelectric particles and carbon black (2.0 vol.% of composite) at a volume ratio of 7:1, the thermoelectric power is increased from 8 to 163 μV/K, the electrical resistivity is decreased from 0.17 to 0.02 Ω.cm, the thermal conductivity is decreased from 1.31 to 0.51 W/m.K, and the dimensionless thermoelectric figure of merit ZT at 70 °C is increased from 9×10^{-6} to 9×10^{-2}. The presence of these fillers causes the carbon fiber content to decrease from 69 to 53 vol.%. Decrease in the curing pressure from 4.0 to 0.5 MPa decreases ZT of the unmodified composite from 9×10^{-6} to 3×10^{-7}, mainly due to the increase in resistivity. Carbon black as the sole filler essentially does not affect the thermoelectric power, but decreases the electrical resistivity. Tellurium increases the thermoelectric power and the electrical resistivity. Bismuth telluride causes the thermoelectric power to be negative [17] and decreases the electrical resistivity. Increase in the bismuth telluride proportion (minority) relative to the tellurium proportion (majority) monotonically decreases the thermoelectric power, the electrical resistivity and
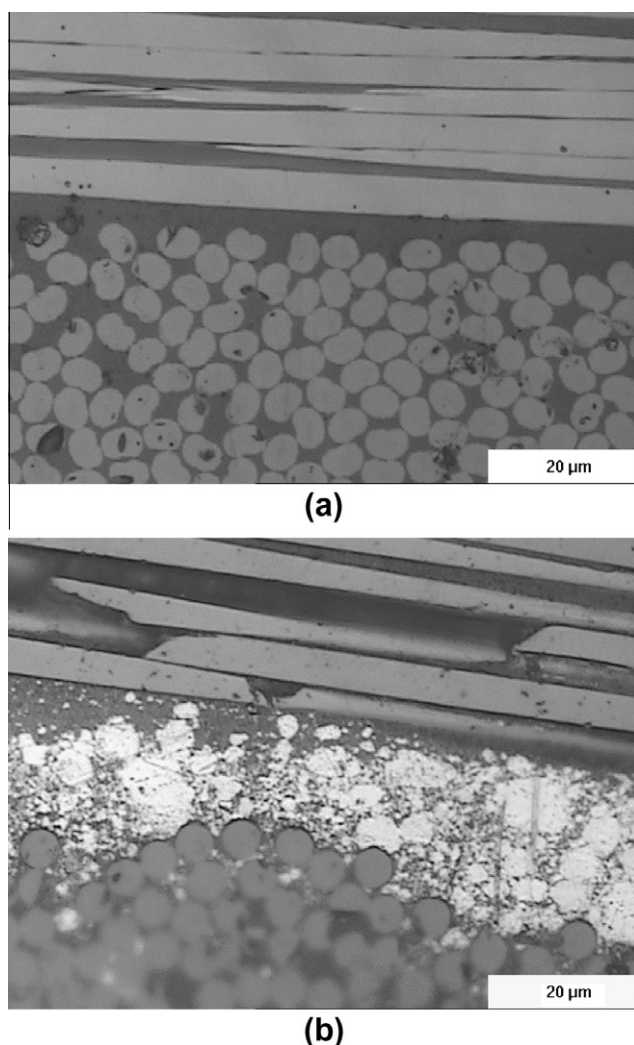
the thermal conductivity, such that ZT is increased. The thermo-electric particle size affects the thermoelectric power and the resistivity, such that, in the presence of carbon black, the intermediate particle size of 8 μm gives the best thermoelectric performance.

References

[1] Sootsman JR, He J, Dravid VP, Li C, Uher C, Kanatzidis MG. High thermoelectric figure of merit and improved mechanical properties in melt quenched PbTe–Ge and PbTe–Ge$_{1-x}$Si$_x$ eutectic and hypereutectic composites. J Appl Phys 2009;105:083718.

[2] Ahn K, Li C, Uher C, Kanatzidis MG. Improvement in the thermoelectric figure of merit by La/Ag cosubstitution in PbTe. Chem Mater 2009;21:1361–7.

[3] Ji X, Zhang B, Su Z, Holgate T, He J, Tritt TM. Nanoscale granular boundaries in polycrystalline Pb 075 Sn 0.25 Te: an innovative approach to enhance the thermoelectric figure of merit. Phys Status Solidi 2009;A206(2):221–8.

[4] Yu F, Zhang J, Yu D, He J, Liu Z, Xu B, et al. Enhanced thermoelectric figure of merit in nanocrystalline Bi$_2$Te$_3$ bulk. J Appl Phys 2009;105:094303.

[5] Ma Y, Hao Q, Poudel B, Lan Y, Yu B, Wang D, et al. Enhanced thermoelectric figure-of-merit in p-type nanostructured bismuth antimony tellurium alloys made from elemental chunks. Nano Lett 2008;8(8):2580–4.

[6] Wang XW, Lee H, Lan YC, Zhu GH, Joshi G, Wang DZ, et al. Enhanced thermoelectric figure of merit in nanostructured n-type silicon germanium bulk alloy. Appl Phys Lett 2008;93:193121.

[7] Rodriguez JE, Lopez J. Thermoelectric figure of merit of oxygen-deficient YBCO perovskites. Physica 2007;387B:143–6.

[8] Rodriguez JE, Cadavid D, Moreno LC. Thermoelectric figure of merit of LSCoO–Mn perovskites. Microelectron J 2008;39:1236–8.

[9] Shi X, Kong H, Li C, Uher C, Yang J, Salvador JR, et al. Low thermal conductivity and high thermoelectric figure of merit in n-type Ba$_x$Yb$_y$Co$_4$Sb$_{12}$ double-filled skutterudites. Appl Phys Lett 2008;92:182101.

[10] Kurosaki K, Goto K, Muta H, Yamanaka S. Enhancement of thermoelectric figure of merit of AgTlTe by tuning the carrier concentration. J Appl Phys 2007;102:023707.

[11] Sekimoto T, Kurosaki K, Muta H, Yamanaka S. High-thermoelectric figure of merit realized in p-type half-Heusler compounds: ZrCoSn$_x$Sb$_{1-x}$. Jap J Appl Phys 2007;46(7):L673–5.

[12] He Z, Stiewe C, Platzek D, Karpinski G, Muller E, Li S, et al. Nano ZrO$_2$/CoSb$_3$ composites with improved thermoelectric figure of merit. Nanotechnology 2007;18:235602–6.

[13] Hiroshige Y, Ookawa M, Toshima N. Thermoelectric figure-of-merit of iodine-doped copolymer of phenylenevinylene with dialkoxyphenylenevinylene. Synth Met 2007;157:467–74.

[14] Pereira T, Guo Z, Yamazaki T, Hahn HT. Development of multifunctional structural composites for energy harvesting. In: Proceedings american society for composites, technical conference, 23rd. DEStech Publications; 2008. p. 97/1–/9.

[15] Wang S, Chung DDL. Carbon fiber polymer–matrix composite interfaces as thermocouple junctions. Compos Interf 1999;6(6):519–30.

[16] Guerrero VH, Wang S, Wen S, Chung DDL. Thermoelectric property tailoring by composite engineering. J Mater Sci 2002;37(19):4127–36.

[17] Han S, Chung DDL. Through-thickness thermoelectric power of carbon fiber polymer–matrix structural composite and decoupled contributions from lamina and interlaminar interface. Carbon 2013;52:30–9.

[18] Han S, Chung DDL. Increasing the through-thickness thermal conductivity of carbon fiber polymer–matrix composite by curing pressure increase and filler incorporation. Compos Sci Technol 2011;71(16):1944–52.

[19] Wang S, Kowalik DP, Chung DDL. Self-sensing attained in carbon fiber polymer–matrix structural composite by using the interlaminar interface as a sensor. Smart Mater Struct 2004;13(3):570–92.

[20] Gao L, Thostenson ET, Zhang Z, Chou T. Sensing of damage mechanisms in fiber-reinforced composites under cyclic loading using carbon nanotubes. Adv Funct Mater 2009;19(1):123–30.

[21] Han S, Lin JT, Aoyagi Y, Chung DDL. Enhancing the thermal conductivity and compressive modulus of carbon fiber polymer–matrix composites in the through-thickness direction by nanostructuring the interlaminar interface with carbon black. Carbon 2008;46(7):1060–71.

[22] Leong C, Chung DDL. Carbon black dispersions as thermal pastes that surpass solder in providing high thermal contact conductance. Carbon 2003;41(13):2459–69.

[23] Leong C, Chung DDL. Carbon black dispersions and carbon–silver combinations as thermal pastes that surpass commercial silver and ceramic pastes in providing high thermal contact conductance. Carbon 2004;42(11):2323–7.

[24] Kumashiro K, Hirata K, Sato K, Yokoyama T, Aisu T, Ikeda T, et al. Thermoelectric properties of boron and boron phosphide films. J Solid State Chem 2000;154(1):26–32.

[25] Yasukawa M, Murayama N. High-temperature thermoelectric properties of the sintered Bi$_2$Sr$_2$Ca$_{1-x}$Y$_x$Cu$_2$O$_y$ (x = 0–1). J Mater Sci 2000;35(13):3409–13.

[26] Shin W, Murayama N. Thermoelectric properties of (Bi, Pb)–Sr–Co–O oxide. J Mater Res 2000;15(2):382–6.

[27] Moon J, Seo W, Okabe H, Okawa T, Koumoto K. Ca-doped RCoO$_3$ (R = Gd, Sm, Nd, Pr) as thermoelectric materials. J Mater Chem 2000;10(9):2007–9.

[28] Moon J, Seo W, Okabe H, Okawa T, Koumoto K. Perovskite-type rare-earth cobalt oxides as thermoelectric materials. In: Int conf thermoelectrics 19th. 2000, p. 147–50.

[29] Pitschke W, Werner J, Behr G, Koumoto K. Structure and thermoelectric properties of Me-substituted In$_4$Sn$_3$O$_{12}$, Me = Y and Ti. J Solid State Chem 2000;153(2):349–56.

[30] Umemoto M, Liu ZG, Omatsuzawa R, Tsuchiya K. Production and characterization of Mn–Si thermoelectric material. Mater Sci Forum 2000;343–346(Pt. 2, Metastable, Mechanically Alloyed and Nanocrystalline Materials):918–23.

[31] Tagiyev MM. High-temperature magnetothermoelectrical extruded material on the basis of Bi85Sb15 solid solution. In: Proceedings of SPIE-the international society for optical engineering 4340 (photoelectronics and night vision devices). 2000, p. 344–7.

[32] Alekseeva GT, Vedernikov MV, Gurieva EA, Prokof'eva LV, Ravich Yu I. Hole concentration and thermoelectric figure of merit for Pb$_{1-x}$Sn$_x$Te:Te solid solutions. Semiconductors (Translation of Fizika i Tekhnika Poluprovodnikov (Sankt-Peterburg) 2000;34(8):897–901.

[33] Yang JY, Aizawa T, Yamamoto A, Ohta T. Preparation and thermoelectric properties of n-type (Bi$_2$Se$_3$)$_x$(Bi$_2$Te$_3$)$_{1-x}$ via bulk mechanical alloying and hot pressing. In: Int conf thermoelectrics 19th. 2000, p. 74–7.

[34] Yang JY, Aizawa T, Yamamoto A, Ohta T. Thermoelectric properties of n-type (Bi$_2$Se$_3$)$_x$(Bi$_2$Te$_3$)$_{1-x}$ prepared by bulk mechanical alloying and hot pressing. J Alloys Compd 2000;312(1–2):326–30.

[35] Ferhat M, Nagao J. Thermoelectric properties of Ag$_2$Te$_x$Se$_{1-x}$ ternary compounds. In: AIP conf proc 504 (Space Technology and Applications International Forum, 2000, Pt. 2). 2000, p. 1513–7.

[36] Yang J, Aizawa T, Yamamoto A, Ohta T. Thermoelectric properties of p-type (Bi$_2$Te$_3$)$_x$(Sb$_2$Te$_3$)$_{1-x}$ prepared by bulk mechanical alloying and hot pressing. J Alloys Compd 2000;309(1–2):225–8.

[37] Toshima N, Yan H, Ohta T. Electrically conductive polyaniline films as organic thermoelectric materials. In: Int conf on thermoelectrics 19th. 2000, p. 214–7.

[38] Miyazaki Y, Kudo K, Akoshima M, Ono Y, Koike Y, Kajitani T. Low-temperature thermoelectric properties of the composite crystal [Ca$_2$CoO$_{3.34}$]$_{0.614}$[CoO$_2$]. Jap J Appl Phys Part 2: Lett 2000;39(6A):L531–3.

[39] Dilley NR, Bauer ED, Maple MB, Sales BC. Thermoelectric properties of chemically substituted skutterudites Yb$_y$Co$_4$Sn$_x$Sb$_{12-x}$. J Appl Phys 2000;88(4):1948–51.

[40] Snyder GJ, Caillat T, Fleurial J-P. Thermoelectric properties of the incommensurate layered semiconductor Ge$_x$NbTe$_2$. J Mater Res 2000;15(12):2789–93.

[41] Snyder GJ, Caillat T, Fleurial J-P. Thermoelectric, transport, and magnetic properties of the polaron semiconductor Fe$_x$Cr$_{3-x}$Se$_4$. Phys Rev B 2000;62(15):10185–93.

[42] Nagao J, Ferhat M. Thermoelectric properties of Bi$_{2(1-x)}$In$_{2x}$Te$_3$ ternary samples. In: AIP conf. proc. 504 (Space Technology and Applications International Forum, 2000, Pt. 2). 2000, p. 1494–9.

[43] Goto T, Li J, Hirai T. Microstructure and thermoelectric properties of B-C-Y system composites. Trans Mater Res Soc Jpn 2000;25(1):213–6.

[44] Shelimova LE, Konstantinov PP, Karpinsky OG, Avilov ES, Kretova MA, Fleurial J.-P. New low thermal conductivity materials in chalcogenide systems with homologous series mixed layered tetradymite-like compounds. In: Int conf thermoelectrics 19th. 2000, p. 408–11.

[45] Ohtaki M, Nojiri Y, Maeda E. Improved thermoelectric performance of sintered NaCo$_2$O$_4$ with enhanced 2-dimensional microstructure. In: Int conf thermoelectrics 19th. 2000, p. 190–5.

[46] Chung D, Hogan T, Brazis P, Rocci-Lane M, Kannewurf C, Bastea M, et al. CsBi$_4$Te$_6$. A high-performance thermoelectric material for low-temperature applications. Science (Washington, DC) 2000;287(5455):1024–7.

[47] Sales BC, Chakoumakos BC, Mandrus D. Thermoelectric properties of thallium-filled skutterudites. Phys Rev B 2000;61(4):2475–81.

[48] Yamashita O, Sadatomi N. Thermoelectric properties of Si$_{1-x}$Ge$_x$ (x ⩽ 0.10) with alloy and dopant segregations. J Appl Phys 2000;88(1):245–51.

[49] Harman TC, Taylor PJ, Spears DL, Walsh MP. Thermoelectric quantum-dot superlattices with high ZT. J Electron Mater 2000;29(1):L1–4.

[50] Anno H, Nagamoto Y, Ashida K, Taniguchi E, Koyanagi T, Matsubara K. Effect of Yb filling on thermoelectric properties of Co$_{1-x}$M$_x$Sb$_3$ (M = Pd, Pt) skutterudites. In: Int conf thermoelectrics 19th. 2000, p. 90–3.

[51] Nolas GS, Kaeser M, Littleton IV RT, Tritt TM. High figure of merit in partially filled ytterbium skutterudite materials. Appl Phys Lett 2000;77(12):1855–7.

[52] Anno H, Matsubara K. A new approach to research for advanced thermoelectric materials: CoSb$_3$ and Yb-filled skutterudites. Recent Res Develop Appl Phys 2000;3:47–61.

[53] Chen LD, Kawahara T, Tang XF, Goto T, Hirai T, Dyck JS, Chen W, Uher C. Thermoelectric properties of n-type BayCo$_4$Sb$_{12}$. In: Int conf thermoelectrics 19th. 2000, p. 348–51.